Journal of Molecular Liquids 230 (2017) 652–661

Contents lists available at ScienceDirect

Journal of Molecular Liquids

journal homepage: www.elsevier.com/locate/molliq

Morpholine and piperazine based carboxamide derivatives as corrosion inhibitors of mild steel in HCl medium

Nnaemeka J.N. Nnaji [a], Oguejiofo T. Ujam [b], Nkechi E. Ibisi [c], Julius U. Ani [b], Thereasa O. Onuegbu [d], Lukman O. Olasunkanmi [e,f,g], Eno E. Ebenso [e,f,*]

[a] Department of Chemistry, Federal University Ndufu Alike, Ikwo, Ebonyi State, Nigeria
[b] Department of Pure and Industrial Chemistry, University of Nigeria, Nsukka, Enugu State, Nigeria
[c] Department of Chemistry, Michael Okpara University of Agriculture, Umudike, Abia State, Nigeria
[d] Department of Pure and Industrial Chemistry, Nnamdi Azikiwe University, Awka, Anambra State, Nigeria
[e] Department of Chemistry, School of Mathematical and Physical Sciences, Faculty of Agriculture, Science and Technology, North-West University (Mafikeng Campus), Private Bag X2046, Mmabatho 2735, South Africa
[f] Material Science Innovation and Modelling (MaSIM) Research Focus Area, Faculty of Agriculture, Science and Technology, North-West University (Mafikeng Campus), Private Bag X2046, Mmabatho 2735, South Africa
[g] Department of Chemistry, Faculty of Science, Obafemi Awolowo University, Ile-Ife 220005, Nigeria

ARTICLE INFO

Article history:
Received 6 November 2016
Received in revised form 9 January 2017
Accepted 22 January 2017
Available online 25 January 2017

Keywords:
Carboxamide
Gravimetric
Thermometric
Adsorption
Quantum chemical calculations

ABSTRACT

N-(2-chloroethyl)morpholine-4-carboxamide (NCMC), *N*-(2-chloroethyl)tiomorpholine-4-carboxamide (NCTC) and *N*,*N*-bis(2-chloroethyl)piperazine-1,4-dicarboxamide (NCPD) were studied as corrosion inhibitors for mild steel using atomic absorption spectroscopy (AAS) and gravimetry and thermometry. Results obtained from the three techniques are similar and reveal that the compounds inhibit mild steel corrosion. The inhibition efficiencies increased from 35.6% to 74.9% (NCMC), 44.5% to 82.4% (NCPD) and 52.6% to 90.1% (NCTC) at 30 °C when the inhibitor concentrations increased from 10 μM to 50 μM. The maximum inhibition efficiency values (at 50 μM) decreased to 46.6%, 58.1% and 61.2% for NCMC, NCPD and NCTC respectively, when the temperature was raised to 50 °C. The decrease in inhibition efficiency with increase in temperature suggested predominant physisorption mechanism in metal/inhibitor interactions. The formation of protective films of NCMC, NCPD and NCTC molecules on mild steel surface were confirmed by FTIR and XRD. The order of inhibitive strengths of the molecules is NCTC > NCPD > NCMC. Quantum chemical calculations revealed the prospective sites through which the molecules can interact with mild steel surface and some quantum chemically derived parameters were used to corroborate experimental.

1. Introduction

Many facilities used at the oil and gas refinery plants are made of mild steel. Steel is a major construction material extensively used in chemical and allied industries for material constructions [1]. It has therefore become the most useful metal in human development. The utilization of mild steel in construction and fabrication of industrial facilities is not only due to its optimum strength to mass ratio that fits the strength requirement of many industrial equipment, but also as a result of its ready availability at moderately low cost. Unfortunately, mild steel being an active alloy of iron undergoes corrosion in nearly all environments, most especially acidic environment. Corrosion of metals has both economic and environmental effects that are of great concern to corrosion and corrosion prevention experts. Corrosion products can be hazardous to man, animal and vegetation. El-Melgi [2] believes that corrosion products from various sources including car constructions, bridges and buildings, water pipeline systems and petroleum industries are notable environmental pollutants.

Steel made materials are often used to hold acid, alkali and salt solutions in chemical and allied industries [2]. Acid induced steel corrosion is by far the most common in industries. Industrial processes that lead to steel corrosion by acids include acid pickling, acid cleaning and oil well acidizing [3]. Safety and cost-effective maintenance of steel materials used for these industrial activities are of paramount consideration [4]. Increased metal corrosion resistance can be achieved in various ways, but often at elevated cost. The use of corrosion inhibitors is therefore a more practical and economic alternative [5]. The use of corrosion inhibitors in industries is extensive and broad based [6].

* Corresponding author at: Department of Chemistry, School of Mathematical and Physical Sciences, Faculty of Agriculture, Science and Technology, North-West University (Mafikeng Campus), Private Bag X2046, Mmabatho 2735, South Africa.
E-mail address: Eno.Ebenso@nwu.ac.za (E.E. Ebenso).

http://dx.doi.org/10.1016/j.molliq.2017.01.075
0167-7322/

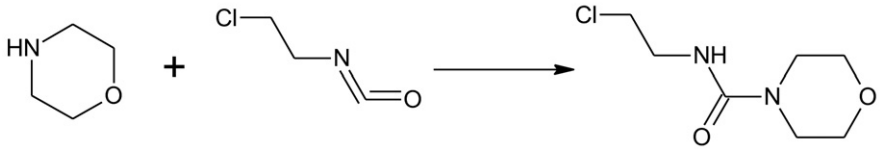

Scheme 1. Synthesis of *N*-(2-chloroethyl)morpholine-4-carboxamide [NCMC].

Though excellent corrosion resistance has been reported for inorganic inhibitors such as chromates, unfortunately, their uses are discouraged due to health and environmental reasons. Notable are the heavy metal based inhibitors which are not favored because of their associated environmental issues. Lanthanide salts, though have low toxicity and good inhibitive properties, are very expensive and their uses are therefore discouraged [7]. Owing to stringent environmental regulations caused by environmental limitations of inorganic inhibitors, and the high cost of less toxic ones, organic compounds are fast replacing inorganic corrosion inhibitors especially the heavy metal derivatives [8].

Carboxamide derivatives are among organic compounds that have been reported in some previous studies as efficient corrosion inhibitors for metals [9–13]. The inhibitive effect of 2-(1-(2-oxo-2h-chromen-3-yl)ethylidene)hydrazinecarboxamide on zinc-aluminium alloy in 1.8 M hydrochloric acid has been reported by Aladesuyi et al. [9]. Paramasivam et al. [10] had reported 4-(pyridin-2yl)-*N*-p-tolylpiperazine-1-carboxamide as effective inhibitor of mild steel corrosion in hydrochloric acid. Zulfareen et al. [11] investigated the inhibitive effect of newly synthesized *N*-(4-morpholinomethylcarbamoylphenyl)-furan-2-carboxamide on corrosion of brass in HCl medium. Shahabi et al. [12] also reported the corrosion inhibition performances of two carboxamide compounds, *N*-{3-methyl-2-[(2-thienylcarbonyl)amino]phenyl}-2-thiophenecarboxamide and *N*-(3-methyl-2-(picolinamido)phenyl)picolinamide for carbon steel corrosion in HCl solution [12].

However, many of these compounds only exhibited high corrosion inhibition performances at relatively high concentrations [10–13] of about 1000 folds higher than what was obtained in the present study. For instance, 4-(pyridin-2yl)-*N*-p-tolylpiperazine-1-carboxamide was used up to 3 mM to obtain inhibition efficiency of about 92% [10]; *N*-(4-morpholinomethylcarbamoylphenyl)-furan-2-carboxamide was used at a concentration as high as 2 mM to get 62% protection performance [11], while *N*-{3-methyl-2-[(2-thienylcarbonyl)amino]phenyl}-2-thiophenecarboxamide and *N*-(3-methyl-2-(picolinamido)phenyl)picolinamide were used at 1 mM to amass 88–91% inhibition efficiency.

In view of the aforementioned, the present work was designed towards the investigation of carboxamides with potentially high inhibition efficiencies at relatively low concentrations. The protection performances of some novel morpholine and piperazine based carboxamide derivatives namely, *N*-(2-chloroethyl)morpholine-4-carboxamide (NCMC), *N*-(2-chloroethyl)thiomorpholine-4-carboxamide (NCTC), and *N*,*N*″″-bis(2-chloroethyl)piperazine-1,4-dicarboxamide (NCPD) for mild steel in HCl medium are hereby reported. Experimental studies were carried out using atomic absorption spectrometry (AAS), gravimetric and thermometric techniques. Density functional theory calculations were also carried out to corroborate experimental findings.

2. Experimental

2.1. Composition of mild steel coupon

Percentages by weight (%) of elemental constituents of mild steel coupon used in corrosion tests are carbon (0.10), manganese (0.54), phosphorus (0.34), sulphur (0.02), silicon (0.26), and iron (98.74).

2.2. Synthesis of the inhibitors (NCMC, NCTC and NCPD)

The synthesis of *N*-(2-chloroethyl)morpholine-4-carboxamide (NCMC) involves the addition of morpholine ($HN(CH_2CH_2)_2O$, 0.174 g, 0.002 mol) to a solution of 2-chloroethylisocyanate ($ClCH_2CH_2NCO$, 0.211 g, 0.002 mol) in dimethylether (30 mL) in a 100 mL round bottom flask. Afterwards, the reaction mixture was stirred for 5 min and a quantitative precipitate of the product, *N*-(2-chloroethyl)morpholine-4-carboxamide, formed immediately. Thereafter, the product was filtered, washed with ether (20 mL), dried under vacuum and characterized using infrared spectroscopic technique. Synthetic technique for NCMC synthesis has been reported elsewhere [14]. NCPD was prepared using piperazine and NCTC using thiomorpholine following similar steps involved in NCMC synthesis. Spectroscopic characterization data of NCMC, NCPD and NCTC have been reported somewhere else [14–16].

The synthetic schemes for the three compounds are summarized in Schemes 1–3.

2.3. Materials

Mild steel sheet was obtained commercially and was mechanically press cut into 5 cm × 4 cm × 0.11 cm coupons for the AAS and gravimetric measurements. Prior to all measurements, the mild steel coupons were successively abraded with emery papers of 240, 400 and 800 grit sizes respectively, degreased in acetone, washed in distilled water and dried. Afterwards, the specimens were put in a desiccator and then used for the respective experiments. Acetone and concentrated hydrochloric acid were of BDH-Analar grades purchased from BDH, Poole, England.

NCMC was dissolved in 10 mL methanol and made up to mark in a 2 L standard flask using hydrochloric acid solution. In 2 L standard flasks, NCTC and NCPD were dissolved in 10 mL of hydrochloric acid solution and made up to mark using same solution. From the stock solutions in the 2 L standard flasks, different concentrations (10–50 μM) of NCMC, NCTC and NCPD were prepared from the stock solutions.

2.4. Weight loss/gravimetric technique

The gravimetric technique used here has been reported earlier [15–18]. Briefly stated, gravimetric measurements were taken by suspending mild steel coupons stored in a desiccator. These coupons were weighed

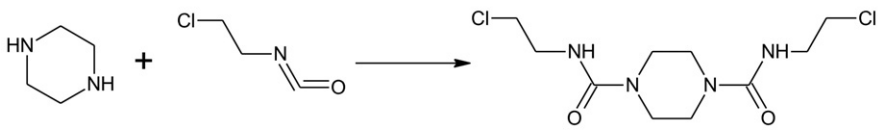

Scheme 2. Synthesis of *N*,*N*″″-bis(2-chloroethyl)piperazine-1,4-dicarboxamide [NCPD].

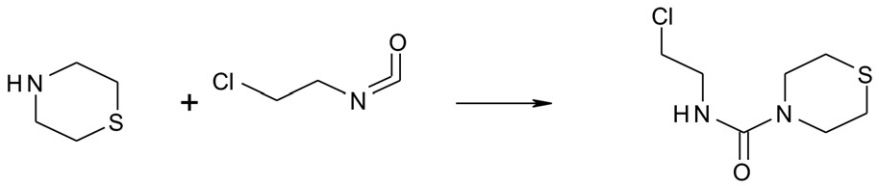

Scheme 3. Synthesis of *N*-(2-chloroethyl)thiomorpholine-4-carboxamide [NCTC].

and immersed completely in 100 mL of 0.5 M HCl in three 250 mL beakers. Also, weighed coupons were completely immersed in 100 mL of 0.5 M HCl solutions containing different concentrations (10, 20, 30, 40 and 50 μM) of each inhibitor. Fifteen setups were made in 250 mL beakers for each inhibitor sample. These represent triplicate gravimetric measurements for each concentration of each inhibitor molecule. Two sets of these were placed in a thermostated oven such that each set was maintained at 30 °C and 50 °C at different times. The coupons were retrieved at 24 h interval for seven days, washed with bristle brush in distilled water at room temperature, dried in acetone and weighed. The difference in weight of the coupons were taken as the weight loss (ΔW) due to corrosion and used to calculate corrosion rate (C_{corr}) by [18]:

$$C_{corr} = \frac{W_1 - W_2}{At} \tag{1}$$

where A is the area of the mild steel coupons (5 cm × 4 cm), and t is the immersion period. The percentage inhibition efficiency (%I) values were calculated using [18]:

$$\%I = \frac{C_1 - C_2}{C_1} \times 100 \tag{2}$$

where C_1 and C_2 are the corrosion rates for mild steel in the absence and presence of inhibitor respectively in HCl solution at the same temperature. The degree of surface coverage (θ), is given by the equation [15,19,20]:

$$\theta = {}^{\%I}\!/_{100} \tag{3}$$

2.5. Thermometric measurements

Mild steel sheet was obtained commercially and was mechanically press cut into 3 cm × 3 cm × 0.11 cm coupons for the thermometric techniques. Prior to all measurements, the mild steel coupons were abraded with emery papers 240, 400 and 800 grit respectively, degreased in acetone, washed in distilled water and dried. Afterwards, the specimens were put in a desiccator and then used for experiments/measurements. The reaction vessel and procedure for determining the corrosion behaviour by this method has been described elsewhere [21]. All experiments were initially carried out at room temperature (30 ± 1 °C) for HCl solutions with and without the inhibitors and this method has been reported earlier [22]. Temperature was read every 2 min as mild steel dissolves in the various acid solutions using mercury in glass thermometer (0–100 °C) read to the nearest ±0.05 °C. Triplicate measurements were performed and the data were reasonably reproducible. This method allowed for the evaluation of the reaction number (RN), defined as [23]:

$$RN\left({}^{°C}\!/_{min}\right) = \frac{T_m - T_i}{t} \tag{4}$$

where T_m and T_i (°C) are maximum and initial temperatures of the system respectively and t (min) is the time taken to reach the maximum temperature.

The percent inhibition efficiency (%I) was evaluated using the equation [23]:

$$\%I = \frac{RN_{aq} - RN_{in}}{RN_{aq}} \times 100 \tag{5}$$

where RN_{aq} is the reaction number calculated for systems without the inhibitors and RN_{in} is the reaction number calculated for systems with the inhibitors. The degree of surface coverage (θ) is given by the equation [18]:

$$\theta = \frac{RN_{aq} - RN_{in}}{RN_{aq}} \tag{6}$$

2.6. AAS measurements and X-ray diffraction characterizations

For the uninhibited and inhibited samples, the amount of iron dissolved in solution was determined using an atomic absorption spectrometer after gravimetric measurements. Triplicate measurements were made based on the experimental setups for gravimetric measurements. The inhibition efficiency was calculated using the equation [18]:

$$\%I = \frac{C_0 - C}{C_0} \times 100 \tag{7}$$

where C_0 (mg L^{-1}) and C (mg L^{-1}) are iron concentrations after immersion in hydrochloric acid solution without and with inhibitor respectively.

Metal surfaces after immersion in hydrochloric acid solutions containing inhibitors were carefully scrapped with potassium bromide (KBr) thoroughly, made into pellets and using the FTIR technique, the spectra of the films were obtained on a SHIMADZU-FTIR-8400S spectrophotometer.

The nature of the metal surfaces both immersed and unimmersed in hydrochloric acid solutions were examined using X-ray diffractometer (EMPYREAN model).

2.7. Statistical analyses

Experimental and theoretical surface coverage values were compared using chi-square (χ^2) statistics according to the following [15]:

$$\chi^2 = \sum \frac{(\theta_{exp} - \theta_{cal})^2}{\theta_{cal}} \tag{8}$$

This comparison is necessary so as to ascertain the adsorption isotherm which gave the best description of the adsorption phenomenon.

The effects of inhibitor type/structure, temperature and inhibitor concentration on inhibition efficiency were investigated and the data analyzed for significance, using Statistical Package for the Social Science (SPSS) version 21.

2.8. Quantum chemical calculations

Initial structures of the molecules were modeled with the aid of GaussView 5.0 and used as input geometry for density functional theory

(DFT) calculations. Gas phase geometry optimizations and frequency calculations were carried out at B3LYP/6-31++G(d,p) level of theory with the aid of Gaussian 09 software [24]. Force constant calculations yielded only real frequencies, suggesting that the optimized structures are equivalent to true energy minima. Frontier molecular orbital (FMO) energies and some derivable parameters were determined for the optimized geometries. Gas phase optimized molecular structures and FMO graphical images were visualized using GaussView 5.0.

3. Results and discussions

3.1. AAS, gravimetric and thermometric techniques

3.1.1. Atomic absorption spectrophotometry (AAS)

Mild steel corrosion in 0.5 M HCl solution alone and solutions containing NCMC, NCTC and NCPD as inhibitors were studied using the AAS technique at 30 °C. AAS was used to determine the amount of iron from the metal into the electrolyte in the absence and presence of the inhibitors after 72 h of immersion. Results reveal that a decrease in the amount of dissolved iron in the presence of the inhibitors was observed compared to the solution without the inhibitors. The inhibition efficiency values for mild steel corrosion inhibition by the inhibitors are shown in Fig. 1. Inhibition efficiency values obtained from AAS technique, after 72 h of immersion, are 64.4%, 73.6% and 86.05% for NCMC, NCPD and NCTC respectively. Results are consistent with the observed trend from other techniques (gravimetry and thermometry) and shows that NCTC protected mild steel best than the other inhibitors within the limit of the concentration studied and at 30 °C.

3.1.2. Gravimetry

The gravimetric technique is a simple and easily available method of investigating metal corrosion, therefore, its practical application is broad [18]. Fig. 2a and b show the inhibition efficiencies of the studied inhibitors, from gravimetric technique, at 30 °C and 50 °C within the concentration range of 10–50 μM. Results reveal that the inhibitors act as good corrosion inhibitors for mild steel in 0.5 M HCl solution. Fig. 2a and b reveal that inhibition efficiencies of the inhibitors decreased with rise in temperature from 30 °C to 50 °C. Increasing inhibitor concentration from 10 μM to 50 μM caused the inhibition efficiencies of the inhibitors to increase. For example, the percentage inhibition efficiency values of 74.9%, 82.4% and 90.1% were obtained at the highest concentration for NCMC, NCPD and NCTC respectively at 30 °C. At 50 °C, the percentage inhibition efficiency values decreased respectively to 46.6%, 58.1% and 61.2% (at 50 μM) for NCMC, NCPD and NCTC. The observed decrease in inhibition efficiency values of the inhibitors at higher temperature suggest possible desorption of some of the adsorbed inhibitor from the surface of the metal. This trend can be ascribed to physical adsorption of the inhibitors onto the metal surface [25]. Comparing inhibition efficiency values, Fig. 2a and b reveals that the performances of the inhibitors are in the following order: NCTC > NCPD > NCMC. Results suggest that the difference in the structural compositions of the inhibitors is such that: the presence of sulphur in the ring system of NCTC caused it to inhibit mild steel corrosion best, NCPD has more nitrogen atoms in its structural make up than NCMC, and NCMC has an oxygen atom in its ring system in place of a nitrogen atom which caused it to perform least in the inhibition process. It can therefore be opined that sulphur, nitrogen and oxygen containing inhibitors perform in the following order S > N > O for mild steel corrosion inhibition. This is in excellent agreement with findings elsewhere [26].

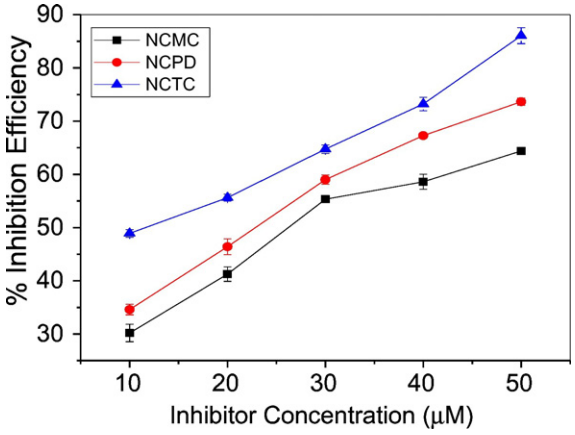

Fig. 1. Inhibition efficiency for mild steel in 0.5 M HCl in the presence of the inhibitors at 30 °C by AAS technique.

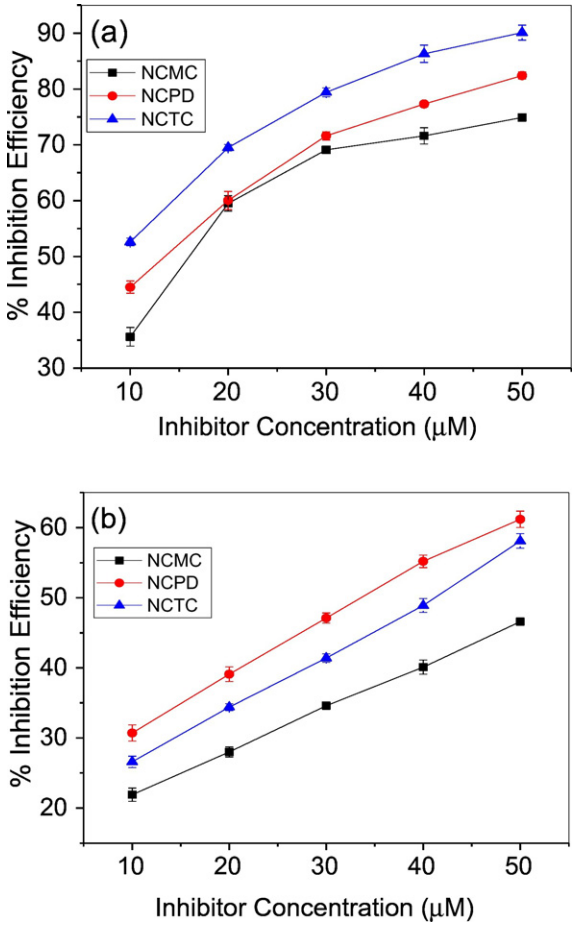

Fig. 2. Inhibition efficiency for mild steel in 0.5 M HCl in the presence of the inhibitors by gravimetric technique at: (a) 30 °C and (b) 50 °C.

For the three inhibitors tested, the level of significance of the effects of temperature and inhibitor concentration was analyzed statistically using analysis of variance (ANOVA) at 95% confidence level. The decision for statistical inference was based on the premise that the value of significance test equal to or greater than 0.05 for tested variables/factors are considered not significant at 95% confidence level. However, when the value of significance test is less than 0.05, the factor is considered significant at 95% confidence level. Table 1 presents values of significance which are less than 0.05 suggesting that the observed variations in values of inhibition efficiency due to the variables (or factors) are significant. Table 1 also presents mean square values which are higher for effect of temperature than for effect of inhibitor concentration, suggesting that the effectiveness of the studied inhibitors is more affected by change in temperature than change in concentration.

Table 1
ANOVA results on the effects of temperature and inhibitor concentration on inhibition efficiency.

Inhibitor	Source	Sum of squares	df	Mean square	F	Significance
NCMC	Temperature	1944.574	1	1944.574	57.230	0.002
	Concentration	1255.179	4	313.795	9.235	0.027
	Residuals	135.913	4	33.978		
	Total	3335.666	9			
NCPD	Temperature	1596.306	1	1596.306	140.718	0.000
	Concentration	1477.802	4	369.451	32.568	0.003
	Residuals	45.377	4	11.344		
	Total	3119.485	9			
NCTC	Temperature	2093.086	1	2093.086	250.190	0.000
	Concentration	1470.343	4	367.586	43.938	0.001
	Residuals	33.462	4	8.366		
	Total	3596.891	9			

3.1.3. Thermometry

Similar to an earlier report [22], Fig. 3 presents inhibition efficiency results gotten for thermometric technique without and with the inhibitors (NCMC, NCPD and NCTC). A striking observation from Fig. 3 is that temperature measured for 2.0 M HCl without NCMC was highest (36 °C and not shown here) when compared to temperatures measured for 2.0 M HCl solutions containing NCMC at different concentrations. This possibly suggests that the presence of NCMC inhibited the mild steel corrosion in hydrochloric acid. Similar results have been reported by Umoren et al. [27]. Results of similar trends with those of NCMC were obtained for NCPD and NCTC. Fig. 3 presents plots of calculated inhibition efficiency values (using Eq. (6)). Comparing inhibitor efficiency values, Fig. 3 reveals that the performance of the inhibitors are in the following order: NCTC > NCPD > NCMC.

3.2. Adsorption considerations

To account for the nature of adsorption of NCMC, NCTC and NCPD onto mild steel in hydrochloric acid, adsorption isotherm which describes the adsorption profile was determined. To achieve this, the adsorption data at 30 °C and 50 °C were fitted into linear adsorption isotherm represented by the following:

$$C/\theta = 1/K_L + C \tag{9}$$

$$\ln\theta = \ln K_F + 1/n \ln C \tag{10}$$

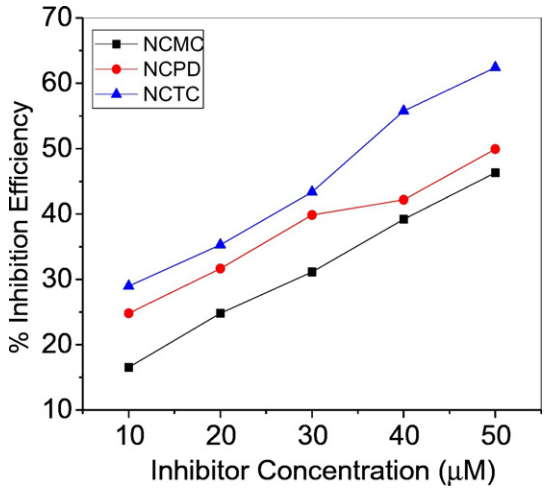

Fig. 3. Inhibition efficiency for mild steel in the presence of the inhibitors by thermometric technique at 30 °C.

$$\theta = 1/f(\ln K_T + \ln C) \tag{11}$$

$$\ln\left[\theta/(1-\theta)\right] = \ln K_{El} + Y_{El} \ln C \tag{12}$$

where Eqs. (9)–(12) represent Langmuir, Freundlich, Temkin and El-Awady adsorption isotherms [15–17]. Symbols presented by the adsorption isotherm equations are: the degree of surface coverage (θ), adsorption capacity values (K_L, K_F, K_T and K_{El}) and adsorption parameters (1/n and Y) which aid to characterize the nature of inhibitor adsorption.

Fig. 4 presents plots of Langmuir, Freundlich, Temkin and El-Awady isotherms for adsorption of inhibitors onto mild steel surface at 30 °C. The corresponding plots at 50 °C are shown in Fig. 5. All the plots show very good fits with almost unity values of R^2 in each case. The observed variations in the slopes of the isotherms at different temperatures suggest interactions among inhibitor species on the metal surface and changes in the adsorption heat with increasing surface coverage. The equilibrium constants for the isotherm plots, i.e. Langmuir (K_L), Freundlich (K_F), Temkin (K_T), and El-Awady (K_E) are listed in Table 2. The values of K_L are all large and positive suggesting strong attractive interactions. The values of K_L at 30 °C are greater than the respective values at 50 °C, implying that increase in temperature decreases the adsorption capacity of the inhibitor molecules. This is characteristic of physisorption mechanism.

The values of K_F for the three compounds at both temperatures are greater than unity, suggesting strong adsorption of the inhibitors on metal surface. The adsorption parameter, n derived from the slope of Freundlich isotherm plots gave values that are greater than unity. This suggests multilayer adsorption, which again supports physisorption mechanism.

Temkin adsorption parameter (f) have the values of 0.2442 M^{-1}, 0.2383 M^{-1} and 0.2365 M^{-1} for NCMC, NCPD and NCTC respectively at 30 °C, and 0.1491 M^{-1}, 0.1887 M^{-1} and 0.1865 M^{-1} for NCMC, NCPD and NCTC respectively at 50 °C. The trend of these values suggest decreased adsorption properties of the inhibitors with increasing temperature. This observation also conforms with physical adsorption mechanism. Large values of Temkin equilibrium adsorption constants (K_T) (Table 2) are indicate strong interactions between inhibitor molecules and the metal surface. K_T values are also larger at lower temperature than higher temperature. The values of El-Awady equilibrium constants (K_E) in Table 2 are also greater than unity, which is in agreement with the inference of strong metal/inhibitor interactions derived from the other isotherm models.

Theoretical surface coverage values derived from the empirical equations of the isotherm plots in Figs. 4 and 5 were plotted against concentration and compared with experimental surface coverage/concentration profiles (Supplementary information Figs. S1, S2 and S3). At 30 °C Temkin isotherm seems to give the best description of the adsorption of NCPD and NCTC, while the adsorption of NCMC was best accounted for by the El-Awady isotherm. At 50 °C, Freundlich isotherm gave the best description for the adsorption of the three compounds. These observations suggest that the adsorption mechanisms (or interaction patterns) of the inhibitors onto metal surface is affected by change in temperature.

3.3. Analyses of the FTIR spectra and X-ray diffraction patterns

3.3.1. Analyses of the FTIR spectra

NCMC has been synthesized earlier [14] and characterized by X-ray diffraction technique. In this report, the FTIR spectra of NCMC, NCPD and NCTC before and after mild steel immersion are presented in Fig. 6. Analyses of FTIR spectra of NCMC revealed a sharp and high intensity signal at 3313 cm^{-1} ascribed to the N—H stretching vibration of

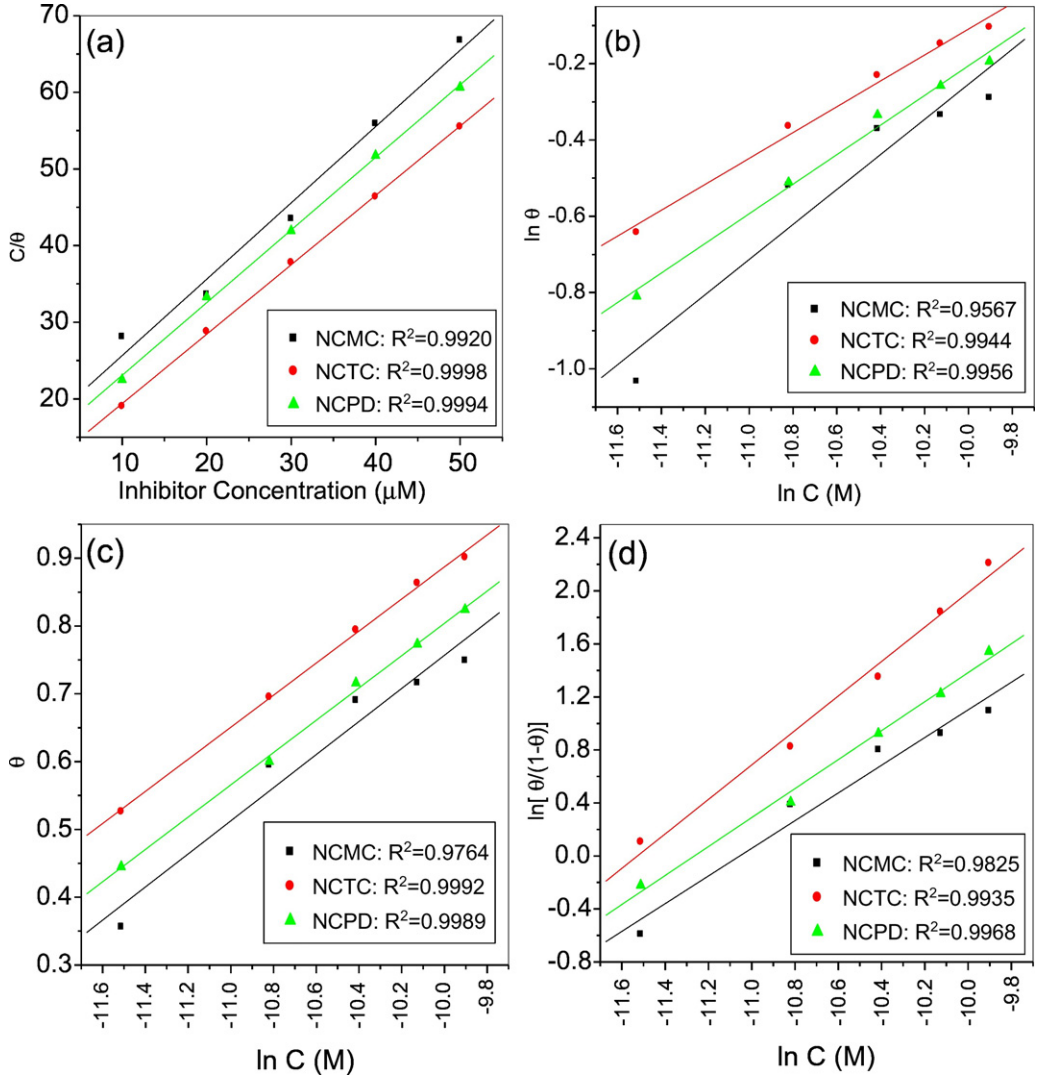

Fig. 4. (a) Langmuir, (b) Freundlich, and (c) Temkin and El-Awady adsorption isotherm plots at 30 °C. (Surface coverage data were taken from gravimetric measurements).

amide group [28] in the pure compound. This signal shifted and was observed as a new peak at 3434 cm^{-1} after corrosion. Weak signals observed in pure NCMC spectra at 2979 cm^{-1}, 2924 cm^{-1} and 2871 cm^{-1} are consistent with CH_2 (stretching) vibrations [29,30], most likely the CH_2 units of the morpholine ring. These weak signals shifted to 2062 cm^{-1} after steel immersion. A high intensity peak at 1626 cm^{-1} corresponds to the vibrational stretching frequency of amide C═O functional group [31] in pure NCMC. This peak shifted to 1639 cm^{-1} in the adsorbed film. A very prominent signal at about 1539 cm^{-1} due to vibration of N—H and C—N of amides [28] was observed in pure NCMC but disappeared in the adsorbed film. Vibrational signal ascribed to alkyl C—H vibration was seen at 1416 cm^{-1} [30], while those corresponding to C—O vibrational signals of morpholine were appeared at 1260 cm^{-1}, 1190 cm^{-1} and 1120 cm^{-1} [30] before steel immersion, but disappeared completely after immersion. At about 1048 cm^{-1}, a weak signal due to C—O—C [31,32] and C—N [29] vibrations was seen in pure NCMC. This signal also disappeared from the adsorbed NCMC film. A group of signals appeared between 956 cm^{-1} and 623 cm^{-1} due to vibrations of morpholine ring [33] in pure NCMC. The region of these signals became very broad, appearing within 1000 cm^{-1} to 500 cm^{-1} range after steel immersion. FTIR spectra of NCMC before and after interaction with mild steel as shown in Fig. 6 suggest that C—O, C═O, C—N, N—CH_2 and N—H are the most likely adsorption sites on NCMC.

The positions of signals in the FTIR spectra of pure NCPD (Fig. 6) are quite similar to that of NCMC except that the spectra of NCPD showed very low intensities. Vibrational signals at 3441 cm^{-1}, 2058 cm^{-1}, 1637 cm^{-1}, and a group of signals within 1000 cm^{-1} to 500 cm^{-1} range corresponding to stretching modes of N—H, C═O, and piperazine ring were observed in the pure NCPD spectra [28]. The signals in the frequency range of 1000 cm^{-1} to 500 cm^{-1} disappeared upon mild steel immersion. The corresponding prominent peaks for C═O and N—H have shifted upon mild steel immersion. These observations suggest that C—O, C═O, C—N, N—CH_2 and N—H groups are probable adsorption sites on NCPD through which the molecule adsorbed on mild steel surface to prevent corrosion.

The infrared spectra of pure NCTC and its adsorbed film on mild steel surface are also shown in Fig. 6. The frequencies and the proposed assignments of vibrations are based on previous assignments. Absorption bands around 3323 cm^{-1} and 3222 cm^{-1} in NCTC before steel immersion, are assigned to N—H vibrations [28]. However, these absorptions shifted to 3442 cm^{-1} after mild steel immersion. Vibrational bands at 1621 cm^{-1} attributed to C═O [31] was observed in pure NCTC, but disappeared in the adsorbed film. The vibrational band at 1532 cm^{-1} for C—N of amide [28] appeared in pure NCTC but disappeared after corrosion. Signals at about 956 cm^{-1}, 823 cm^{-1} and 748 cm^{-1} correspond to C—S [34], C—H (out of plane) [21] and N—CH_2 (rocking) [35] vibrations respectively. Signal at 631 cm^{-1} is due C—S vibration and that

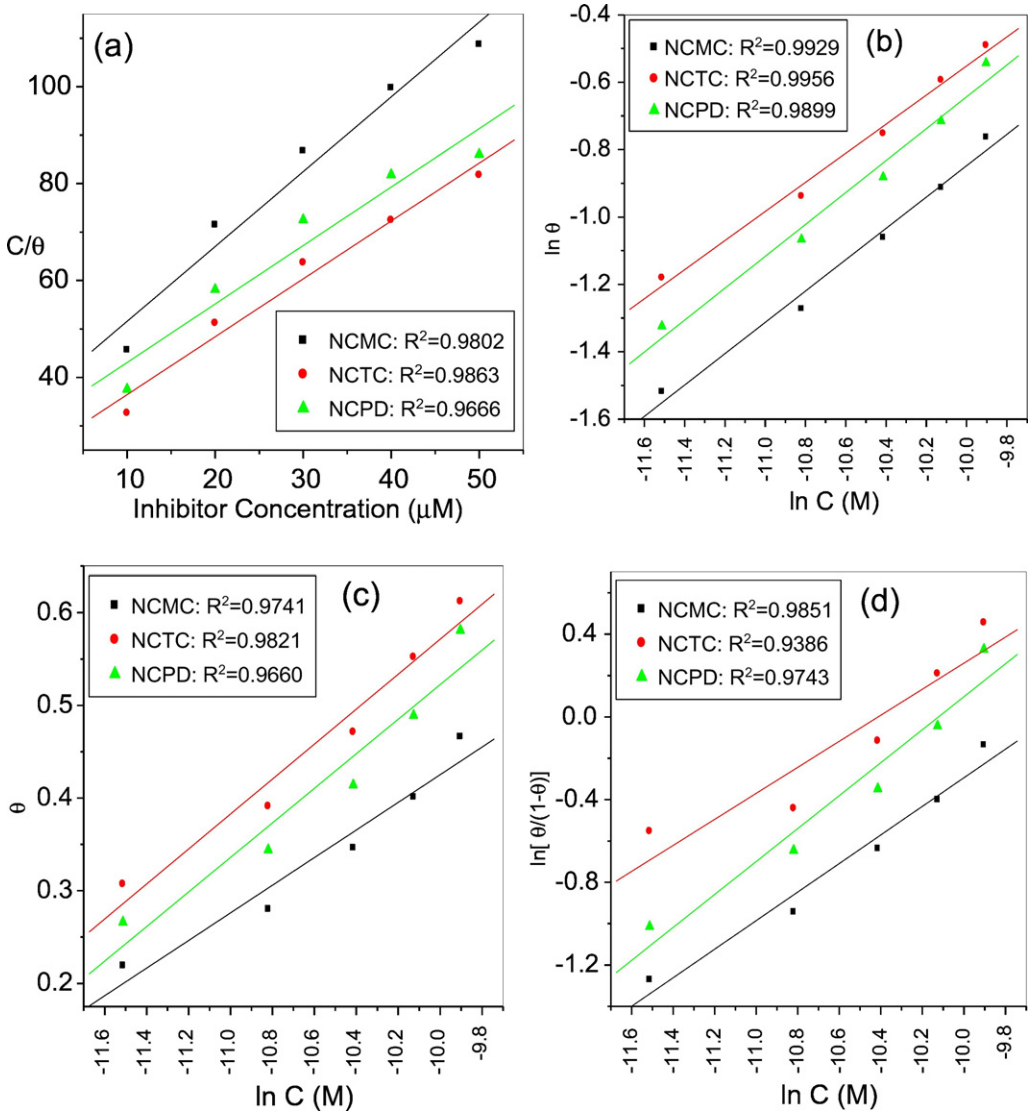

Fig. 5. (a) Langmuir, (b) Freundlich, and (c) Temkin and El-Awady adsorption isotherm plots at 50 °C. (Surface coverage data were taken from gravimetric measurements).

centered at 551 cm^{-1} may be ascribed to C—Cl [36] and C═O (in plane) [35]. After corrosion these signals appear within 1000 cm^{-1} and 500 cm^{-1} range. Evidences from infrared spectra of NCTC before and after corrosion suggest that C—C, C—Cl, C—S, C═O, CH_2—N and N—H segments/regions of NCTC molecule were involved in the adsorption of NCTC onto mild steel surface. Adsorption of NCTC onto mild steel most likely occurred through these sites because of electron distributions in these regions of the molecule. The molecule therefore formed protective layer on metal surface and prevented it from corroding.

Table 2
Adsorption equilibrium constants from Langmuir (K_L), Freundlich (K_F), Temkin (K_T) and El-Awady (K_E) isotherms.

Inhibitor	K_L (L/mol)	K_F	K_T	K_E
30 °C				
NCMC	50,000.00	76.700	488,902.37	103,984.80
NCTC	100,000.00	26.59	939,464.71	3265.75
NCPD	100,000.00	39.36	643,268.88	24.22
50 °C				
NCMC	25,000.00	44.81	381,466.12	747.32
NCTC	33,333.33	43.28	362,023.28	704.79
NCPD	50,000.00	59.81	455,015.57	3193.27

3.3.2. Analyses of the X-ray diffraction patterns

Corrosion inhibition property is widely ascribed to adsorption of inhibitor molecules onto metal surface [37–39]. X-ray diffraction has been used literature [38] to provide supporting evidence of adsorption of inhibitor molecules onto mild steel surface, thereby leading to corrosion inhibition.

In the present study, X-ray diffraction (XRD) patterns were taken of mild steel surface in 0.5 M HCl without and with inhibitors. A sharp peak at about 44 (2θ) for mild steel surface immersed in acid suggests presence of FeOOH formed due to corrosion of the metal [40]. This peak disappeared and broadened peaks within 32 (2θ) to 49 (2θ) appeared for mild steel surfaces immersed in acid solutions containing the inhibitors. New peaks centered at about 23 (2θ) appeared for mild steel surfaces immersed in acid containing inhibitors suggesting the absence of iron oxide peaks possibly due to protection of the metal surfaces by the inhibitors [41]. These observed changes indicate that surface films formed on the mild steel surfaces and that the films are very likely responsible for the protection of the metal surface from corrosion attacks by HCl.

3.4. Quantum chemical studies

Quantum chemical calculations were performed on NCMC, NCPD and NCTC molecules in an attempt to provide molecular and electronic

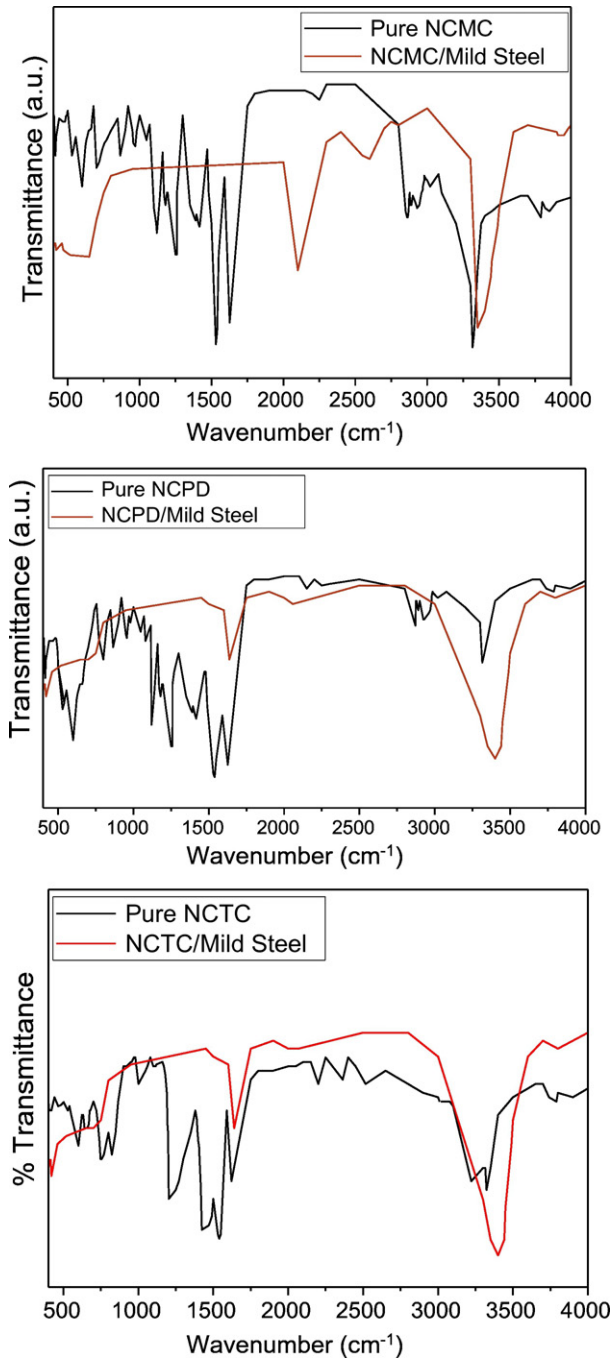

Fig. 6. FTIR spectra of pure NCMC, NCPD, and NCTC, and the corresponding spectra of their adsorbed films on mild steel surface.

based explanations for the corrosion inhibition potentials of the studied inhibitors. The optimized geometries of the molecules are presented in Fig. 7. The optimized structures revealed the twist-boat conformations of morpholine, piperazine and thiomorpholine rings in NCMC, NCPD and NCTC respectively, which is in agreement with literature report [42].

Frontier molecular orbital (FMO) theory is very helpful in accounting for the adsorption centers that are responsible for the interactions of the inhibitors with metal surface. The graphical images of electron density distributions in the FMO highest occupied molecular orbital (HOMO) and lowest unoccupied molecular orbital (LUMO) are presented in Fig. 8. It can be observed from the HOMO graphics that the morpholine, piperazine and thiomorpholine rings in NCMC, NCPD and NCTC

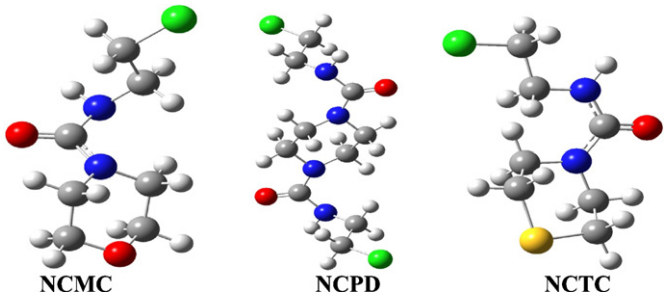

Fig. 7. Gas phase optimized structures of the studied molecules at B3LYP/6-31++G(d,p) level.

respectively, are electron rich centers that can be actively involved in adsorptive interactions with metal surface. On the other hand, the 2-chloroethyl group is a significant contributor to the LUMO in each molecule and could serve as a prospective center through which the molecules can accept charges from appropriate occupied orbitals of a metal.

Some molecular parameters derived from the calculations are listed in Table 3. The HOMO energy (E_{HOMO}), the LUMO energy (E_{LUMO}), and the energy gap (ΔE), global hardness (η), global electronegativity (χ), fraction of electron transferred from inhibitor to metal (ΔN), and dipole moments are reported in Table 3 for the three inhibitor molecules. The derived parameters, ΔE ($\Delta E = E_{LUMO} - E_{HOMO}$), η, χ, and ΔN were calculated as previously reported [43]. These parameters have been suggested to be helpful in explaining the performance of compounds as corrosion inhibitors [15].

The electron donating ability of an inhibitor to appropriate metal (acceptor) with low energy or empty orbital is enhanced by high E_{HOMO} value of the inhibitor molecule. Calculated E_{HOMO} values for the inhibitors as shown in Table 3 revealed that NCTC has the highest E_{HOMO}, which is in support of its highest inhibition efficiency based on enhanced donor ability. Though, NCPD has lower E_{HOMO} than NCMC, its higher inhibition efficiency can be as a result of its lower E_{LUMO} compared to NCMC, which supports better electron accepting ability from the metal. Since adsorption and corrosion inhibition ability of an organic compound is related to donor-acceptor ability, both forward and backward donation of electrons might have effect in inhibitive potential.

Relative reactivity of molecules can be judged from the values of energy gap (ΔE), global hardness (η) and electronegativity (χ). Lower values of ΔE and η imply higher reactivity and vice versa. A molecule with lower value of χ has a poor grip of its molecular electrons and better tendency of releasing electrons in intermolecular interactions. In this regards, the lowest values of ΔE, η and χ for NCTC are all in support of its highest inhibition efficiency. The highest value of ΔN for NCTC also implies that it is has better disposition to donating electrons than NCMC and NCPD. On the other hand, a higher value of χ and lower value of ΔN for NCPD compared to NCMC might inform the higher protection efficiency of the former compared to the latter. The values of dipole moment in Table 3 revealed that NCPD (with dipole moment of 0.00 Debye) has a molecular plane of symmetry and an inversion center. However, the values of the dipole moments for the molecules do not suggest any uniform trend of the inhibitive strengths of the molecules.

3.5. Inhibition mechanism

Morpholine derived carboxamide compounds contain the carboxamide functional group (—CO—NH—) attached to morpholine. Chiu and Lo [44] suggest that amides exist as equilibrium mixtures of the protonated, neutral, and/or deprotonated species in aqueous systems. Although amides may be regarded as neutral compounds [45], the schemes below present the various forms of morpholine derived carboxamide compounds.

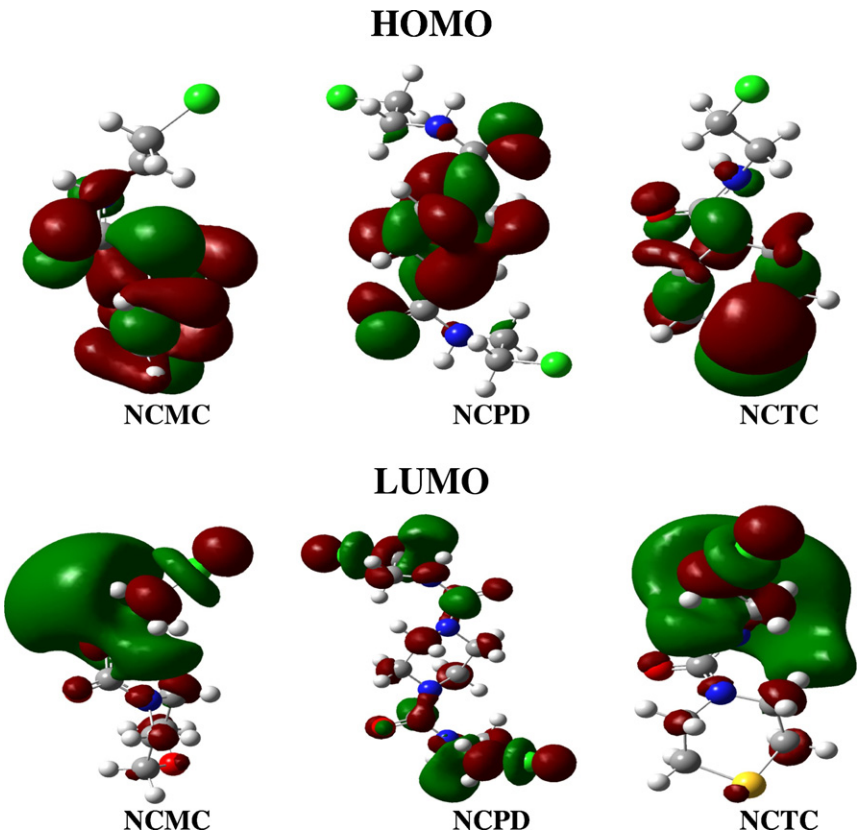

Fig. 8. Highest occupied molecular orbitals (HOMO) of (a) NCMC, (b) NCTC and (c) NCPD.

Meanwhile, in aqueous acidic solutions, mild steel surface possesses positive charge [45,46], and Schemes 4 and 5 show that the inhibitors could be in protonated, neutral and/or deprotonated forms. In protonated forms (structure V), the chloride ions which possess excess negative charges adsorb onto the positively charged mild steel surface by electrostatic interactions. These interactions give rise to a net negative charge which subsequently attracts the protonated form of the inhibitor onto the metal surface. The chloride ions from the acid (HCl) might also aid these electrostatic interactions.

Another possible mechanism of adsorption of the inhibitor molecules on mild steel surface is through donor-acceptor interactions between π-electrons of the carboxamide centers of the inhibitors, the lone pairs of electrons of oxygen and sulphur atoms of morpholine and thiomorpholine centers of the inhibitors, and the vacant d-orbitals of mild steel surface. This possibility of this mechanism is quite revealing in the electron density distributions of the FMOs (vide supra Fig. 8). Similar inhibition mechanism has been reported for elsewhere [46].

4. Conclusions

Newly synthesized *N*-(2-chloroethyl)morpholine-4-carboxamide (NCMC), *N*-(2-chloroethyl)tiomorpholine-4-carboxamide (NCTC) and *N*,*N*-bis(2-chloroethyl)piperazine-1,4-dicarboxamide (NCPD) have been tested as possible inhibitors of mild steel corrosion in HCl using atomic absorption spectroscopy (AAS), gravimetric and thermometric techniques. Theoretical quantum chemical calculations were also carried out on the molecules. Conclusions drawn from the studies are summarized as follows:

- NCMC, NCPD and NCTC inhibit mild steel corrosion in HCl medium and their inhibition efficiencies increase with increasing concentration, and decrease with increase in reaction temperature. Their adsorption on mild surface was inferred to be based on physisorption mechanism.
- Adsorption profiles of NCPD and NCTC were found to obey Temkin adsorption isotherm, but El-Awady adsorption isotherm gave the best fit for the adsorption profile of NCMC onto mild steel surface at 30 °C. Freundlich isotherm, however, gave excellent account of the adsorption patterns of the three compounds at 50 °C. Change in temperature might affect adsorption mode of the compounds.
- FTIR spectroscopic and X-ray diffraction studies reveal that protective films most likely formed on the mild steel surface in the presence of the inhibitors and very possible because of adsorption of the inhibitors on the metal surface. These formed protective films are probably responsible for the retardations of the corrosion processes of the metal in the presence of the inhibitors;
- Theoretical considerations suggest that the corrosion inhibition mechanism which involves the electrostatic interactions between the inhibitor/metal surface interface explains the inhibition mechanism exhibited by NCPD and NCTC. To account for the inhibition mechanism for NCMC, NCPD and NCTC, the acceptor/donor mechanism is the theoretical consideration which explains the adsorption pattern of the studied inhibitors onto mild steel. Quantum chemical calculations strongly support experimental results that the corrosion inhibition performance of the inhibitors is in the order NCTC > NCPD > NCMC

Table 3
Selected quantum chemical parameters for NCMC, NCPD and NCTC obtained at B3LYP/6-31++(d,p) level.

Inhibitor molecule	E_{HOMO} (eV)	E_{LUMO} (eV)	ΔE (eV)	η (eV)	χ (eV)	ΔN	Dipole moment (Debye)
NCMC	−6.675	−0.521	6.154	3.077	3.598	0.553	1.644
NCPD	−7.059	−0.658	6.400	3.200	3.859	0.491	0.000
NCTC	−6.276	−0.546	5.731	2.865	3.411	0.626	1.539

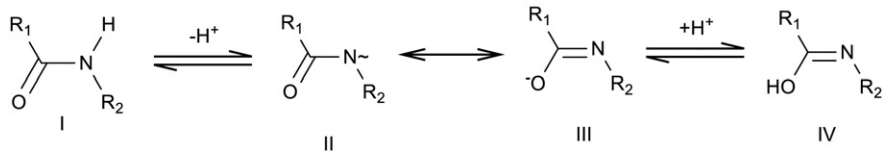

Scheme 4. Carboxamide (I), carboxamide anion (II and III), and carboxamidic acid (IV).

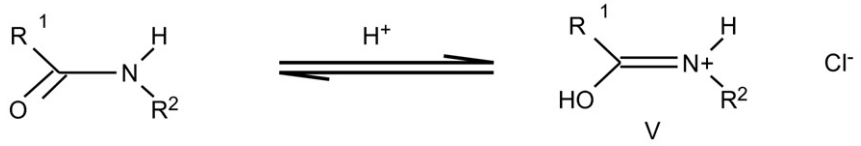

Scheme 5. Protonation of carboxamide.

thus supporting that inhibitors containing sulphur atoms in their structural compositions perform best and those containing nitrogen atoms perform better, then followed by those containing oxygen atoms.

Appendix A. Supplementary data

Supplementary data to this article can be found online at http://dx.doi.org/10.1016/j.molliq.2017.01.075.

References

[1] H.M. Abd El-Lateef, Corros. Sci. 92 (2015) 104–117.
[2] A.A. El-Melgi, Recent Patents Corros. Sci. 2 (2010) 22–33.
[3] M. Finsgar, J. Jackson, Corros. Sci. 86 (2014) 17–41.
[4] B. Bamaiyi, M. Peni, Int. Res. J. Mater. Sci. Eng. 2 (1) (2015) 12–18.
[5] L.T. Popoola, A.S. Grema, G.K. Latinwo, B. Gutti, A.S. Baligun, Int. J. Ind. Chem. 4 (2013) 35.
[6] A.A. Rahim, E. Rocca, J. Steinmetz, M.J. Kassim, R. Adnan, S.N. Ibrahim, Corros. Sci. 49 (2007) 402–417.
[7] R.T. Loto, C.A. Loto, A.P.I. Popoola, J. Mater. Environ. Sci. 3 (5) (2012) 885–894.
[8] B.E.A. Rani, B.B. Basu, Green inhibitors for corrosion protection of metals and alloys: an overview. 10.1155/2012/380217, 2012 (accessed 16.10. 16).
[9] O. Aladesuyi, B.O. Fatile, E.A. Adedapo, A.P. Ogunboyejo, C.O. Ajanaku, I.O. Olarenwaju, O.O. Ajani, K.O. Ajanaku, Int. J. Adv. Res. Chem. Sci. 3 (2) (2016) 1–6.
[10] S. Paramasivam, K. Kulanthai, G. Sadhasivam, R. Subramani, Int. J. Electrochem. Sci. 11 (2016) 3393–3414.
[11] N. Zulfareen, K. Kannan, T. Venugopal, S. Gnanavel, Arab. J. Chem. 9 (1) (2016) 121–135.
[12] Sh. Shahabi, P. Norouzi, M.R. Ganjali, Russ. J. Electrochem. 51 (9) (2015) 833–842.
[13] R. Chen, L. Guo, S. Xu, Int. J. Electrochem. Sci. 9 (2014) 6880–6895.
[14] O.T. Ujam, S.M. Devoy, W. Henderson, B.K. Nicholson, T.S. Andy Hor, Inorg. Chim. Acta 363 (2010) 3558–3568.
[15] C.P. Ozoemena, Synthesis and characterization of isocyanate derivative of [Pt2(u-S)2(PPh3)4]. M.Sc. Thesis, University of Nigeria, Nsukka, Enugu, 2015.
[16] O.T. Ujam, J.N. Asegbeloyin, B.K. Nicholson, P.O. Ukoha, N.N. Ukwueze, Acta. Cryst. Sec. E E70 (2014) o463.
[17] N.J.N. Nnaji, C.O.B. Okoye, N.O. Obi-Egbedi, M.A. Ezeokonkwo, J.U. Ani, Int. J. Electrochem. Sci. 8 (2013) 1735–1758.
[18] U.M. Eduok, S.A. Umoren, A.P. Udoh, Arab. J. Chem. 5 (2012) 325–337.
[19] A.A. El-Shafei, M.N.H. Moussa, A.A. El-Far, J. Appl. Electrochem. 27 (1997) 1075–1078.
[20] I.B. Obot, N.O. Obi-Egbedi, S.A. Umoren, Int. J. Electrochem. Sci. 4 (2009) 863–877.
[21] K. Aziz, A.M. Shams El-Din, Corros. Sci. 5 (7) (1965) 489–501.
[22] S.A. Umoren, I.B. Obot, E.E. Ebenso, N.O. Obi-Egbedi, Desalination 250 (2009) 225–236.
[23] E.E. Ebenso, O. Ogbobe, S.A. Umoren, Trans. SAEST 41 (2006) 74–81.
[24] M.J. Frisch, G.W. Trucks, H.B. Schlegel, G.E. Scuseria, M.A. Robb, J.R. Cheeseman, G. Scalmani, V. Barone, B. Mennucci, G.A. Petersson, Gaussian 09, Revision D.01, Gaussian Inc., Wallingford CT, 2009.
[25] E.E. Oguzie, Corros. Sci. 49 (3) (2007) 1527–1539.
[26] A. Zarrouk, B. Hammouti, A. Dafali, M. Bouachrine, H. Zarrok, S. Boukhris, S.S. Al-Deyab, J. Saudi Chem. Soc. 18 (2014) 450–455.
[27] S.A. Umoren, O. Ogbobe, I.O. Igwe, E.E. Ebenso, Corros. Sci. 50 (2008) 1998–2006.
[28] A. Barth, Biochim. Biophys. Acta 1767 (2007) 1073–1101.
[29] P. Rawat, R.N. Singh, http://dx.doi.org/10/1016/j.arabjc.2014.10.050.
[30] P. Rawat, R.N. Singh, http://dx.doi.org/10/1016/j.arabjc.2015.03.001.
[31] N.J.N. Nnaji, T.U. Onuegbu, O. Edokwe, G.C. Ezeh, A.P. Ngwu, J. Environ. Chem. Eng. 4 (2016) 3205–3216.
[32] S. Basoglu, M. Yolal, A. Demirbas, H. Bektas, R. Abbasoglu, N. Demirbas, Turk. J. Chem. 36 (2012) 37–53.
[33] J.O. Nwadiogbu, P.A.C. Okoye, V.I. Ajiwe, N.J.N. Nnaji, J. Environ. Chem. Eng. 2 (2014) 1699–1704.
[34] M. Nurnabi, M. Ismail, Bangladesh J. Sci. Ind. Res. 42 (2) (2007) 135–146.
[35] S. Jeyavijayan, Spectrochim. Acta A Mol. Biomol. Spectrosc. 136 (B) (2015) 896–899.
[36] A.A.H. Kadhum, A.B. Mohamad, L.A. Hammed, A.A. Al-Amiery, N.H. San, A.Y. Musa, Mat. 7 (2014) 4335–4348.
[37] I.B. Obot, N.O. Obi-Egbedi, S.A. Umoren, Corros. Sci. 51 (2009) 276–282.
[38] M.G. Sethuraman, V. Aishwarya, C. Kamal, T.I.E. Jebakumar, http://dx.doi.org/10/1016/j.arabjc.2012.10.013.
[39] A. Handy, N.S. El-Gendy, Egypt. J. Pet. 22 (2013) 17–25.
[40] A. Singh, Y. Lin, E.E. Ebenso, W. Liu, B. Huang, Int. J. Electrochem. Sci. 9 (2014) 5993–6005.
[41] R. Karthik, P. Muthukrishnan, Shen-Ming Chen, B. Jeyaprabha, P. Prakash, Int. J. Electrochem. Sci. 10 (2015) 3707–3725.
[42] V.L.S. Freitas, J.R.B. Gomes, M.D.M.C. Ribeiro da Silva, J. Chem. Eng. Data 59 (2014) 312–322.
[43] O.L. Olasunkanmi, I.B. Obot, M.M. Kabanda, E.E. Ebenso, J. Phys. Chem. C 119 (2015) 16004–16019.
[44] F.C.K. Chiu, C.M.Y. Lo, J. Am. Soc. Mass Spectrom. 11 (2000) 1061–1064.
[45] B.Z. Volchek, A.V. Purkina, Polym. Sci. USSR 9 (6) (1967) 1403–1409.
[46] I.B. Obot, N.O. Obi-Egbedi, S.A. Umoren, E.E. Ebenso, Int. J. Electrochem. Sci. 5 (2010) 994–1007.